RSC Advances

ROYAL SOCIETY OF CHEMISTRY

www.rsc.org/advances

Graphical abstract

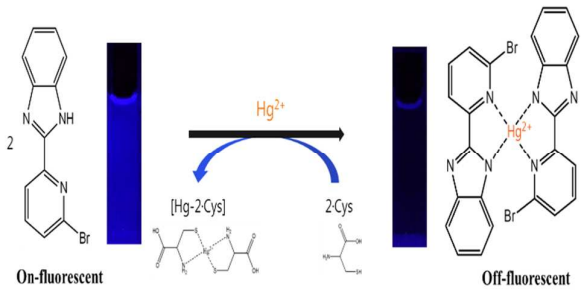

Fluorescent chemosensor showed the sequential detection of Hg^{2+} and cysteine, and could be applied for quantification of Hg^{2+} in water samples.

Fluorescence 'on-off-on' chemosensor for the sequential recognition of Hg^{2+} and cysteine in water

Ye Won Choi, Jae Jun Lee, Ga Rim You, Cheal Kim*

Department of Fine Chemistry and Department of Interdisciplinary Bio IT Materials, Seoul National University of Science and Technology, Seoul 139-743, Korea. Fax: +82-2-973-9149; Tel: +82-2-970-6693; E-mail: chealkim@seoultech.ac.kr

Abstract

A simple fluorescent chemosensor **1** for the sequential detection of Hg^{2+} and cysteine was developed by combination of benzene-1,2-diamine and 6-bromopyridine-2-carboxaldehyde. The sensor **1** exhibited an 'ON-OFF' fluorescent quenching response in the presence of Hg^{2+}, and could be applied for detection of Hg^{2+} with a good recovery in water samples. The sensing mechanism of **1** for Hg^{2+} was supported by theoretical calculations. Moreover, the resulting Hg^{2+}-2·**1** complex acted as an efficient 'OFF-ON' sensor for cysteine, showing recovery of **1** from Hg^{2+}-2·**1** complex. Therefore, the sensor **1** can be employed as a practical fluorescent chemosensor for recognition of Hg^{2+} and cysteine in aqueous solution.

Keywords: chemosensor, mercury ion, cysteine, sequential detection, fluorometric

1. Introduction

There is a considerable concern over the severe risk of heavy metal pollution and poisoning in environment, food and products.[1-10] Mercury ion is of particular interest because it is a deadly toxin to humans by leading to central nervous system defects, erythrism, arrhythmia, cardiomyopathy and kidney damage.[11] The soluble inorganic Hg^{2+} ion is a caustic and carcinogenic material with a high cellular toxicity.[12] Methyl mercury converted by bacteria in the environment subsequently accumulates in animals and plants and also enters into the human body through the food chains.[13,14] As a strong neurotoxin, methyl mercury ions can cause human health problems due to their easy absorption through the skin, respiratory and cell membranes, leading to digestive, cardiac, kidney and DNA damage, mitosis impairment and especially permanent damage to the central nervous system.[15-21] Therefore, developing highly efficient sensors to detect Hg^{2+} ions is important for human health and environmental protection.

Cysteine (Cys) as intracellular thiol plays a prominent role in various critical biological systems such as metabolic processes, biocatalysis and detoxifications of xenobiotics.[22-26] In the human plasma, their abnormal levels have led to some diseases such as Alzheimers disease, cardiovascular disease, neural tube defect, inflammatory bowel disease and osteoporosis.[27-29] Also, a deficiency of Cys is involved in many health problems, including slowed growth in child, hair depigmentation, edema, lethargy, liver damage, muscle and fat loss, skin lesions, and weakness.[30-32] Because of its important roles in biological systems, detecting and monitoring cysteine is very important for environment and human health care.

Till now, various methods, including mass spectrometry (MS), gas chromatography, high-performance liquid chromatography and electrochemical methods, have been employed to detect mercury ion and cysteine.[33-36] However, these methods often require expensive, sophisticated and time consuming procedures. By contrast, fluorescence technology has especially pursued owing to its simplicity, sensitive responses, inexpensive instrument and efficiency.[37-39] Thus, chemosensor based on fluorogenic determination have attracted a considerable attention in the detection of Hg^{2+} and Cys.

Chemosensors based on benzimidazole moiety have, recently, received much attention because of their potential use as fluorescent sensors.[40] The benzimidazole moiety usually shows a strong fluorescence with a π-conjugated system.[41] Additionally, it acts as a selective binding site for cations because of NH and N groups within the imidazole and pyridine rings.[42] Therefore, we designed and synthesized a potential chemosensor **1** based on the benzimidazole moiety, and tested its sensing properties towards various metal ions and, sequentially, amino acids.

Herein, we report a benzimidazole-based fluorescent chemosensor **1**, which was synthesized in one step by condensation reaction of benzene-1,2-diamine and 6-bromopyridine carboxaldehyde. The sensor **1** could detect Hg^{2+} by fluorescence quenching response with high selectivity in water solution. Subsequently, chemosensing ensemble Hg^{2+}-2·**1** showed highly selective detection to Cys via fluorescence enhancement by utilizing the mercury-cysteine affinity. Moreover, **1** sensed quantitatively Hg^{2+} in the water samples.

2. Experimental

2.1 Materials and equipment

All the solvents and reagents (analytical and spectroscopic grade) were purchased from Sigma-Aldrich. ^{1}H and ^{13}C NMR spectra were recorded on a Varian 400 MHz and 100 MHz spectrometer and chemical shifts were recorded in ppm. Electro spray ionization mass spectra (ESI-MS) were collected on a Thermo Finnigan (San Jose, CA, USA) LCQ$_{TM}$ Advantage MAX quadrupole ion trap instrument by infusing samples directly into the source using a manual method. Spray voltage was set at 4.2 kV, and the capillary temperature was at 80 ^{o}C. Absorption spectra were recorded at room temperature using a Perkin Elmer model Lambda 2S UV/Vis spectrometer. The emission spectra were recorded on a Perkin-Elmer LS45 fluorescence spectrometer. Elemental analysis for carbon, nitrogen and hydrogen was carried out using a Flash EA 1112 elemental analyzer (thermo) at the Organic Chemistry Research Center of Sogang University, Korea.

2.2. Synthesis of receptor **1**

An ethanolic solution of benzene-1,2-diamine (0.33 g, 3 mmol) was added to 6-bromopyridine-2-carboxaldehyde (0.19 g, 1 mmol) in ethanol (10 mL). The reaction solution was stirred for 1 d at room temperature. After evaporation, product was purified by column chromatography and dried under vacuum. The yield : 0.18 g (58 %); ^{1}H NMR (400 MHz DMSO-d_6, ppm): δ 13.04 (s, 1H), 8.34 (d, J = 8 Hz, 1H), 7.96 (t, J = 8 Hz, 1H), 7.77 (d, J = 8 Hz, 1H), 7.70 (m, 2H), 7.26 (d, J = 8 Hz, 2H); ^{13}C NMR (100 MHz DMSO-d_6, ppm): 149.64, 148.96, 143.72, 141.13, 140.67, 134.99, 128.80, 123.50, 122.16, 120.77, 119.40, 112.32. ESI-MS m/z (M + H^+): calcd, 274.00; found, 274.20. Anal. Calc. for $C_{15}H_{10}N_4O$: C, 52.58; H, 2.94; N, 15.33. Found: C, 52.58; H, 2.95; N, 15.30%.

2.3. Fluorescence titration

For Hg^{2+}, **1** (1.4 mg, 0.005 mmol) was dissolved in methanol (1 mL) and 0.6 μL of this solution (5 mM) were diluted with 3 mL of 10 mM bis-tris buffer to make the final concentration of 1 μM. $Hg(NO_3)_2{\cdot}H_2O$ (1.7 mg, 0.005 mmol) was dissolved in dimethylformamide (DMF, 1 mL) and 1.2-15 μL of this Hg^{2+} solution (5 mM) were transferred to each receptor solution (1 μM). After mixing them for a few seconds, fluorescence spectra were taken at room temperature.

For Cys, **1** (1.4 mg, 0.005 mmol) was dissolved in methanol (1 mL) and 0.6 μL of this solution (5 mM) were diluted with 3 mL of 10 mM bis-tris buffer to make the final concentration of 1 μM. $Hg(NO_3)_2{\cdot}H_2O$ (1.7 mg, 0.005 mmol) was dissolved in DMF (1 mL) and 15 μL of this Hg^{2+} solution (5 mM) were transferred to each receptor solution (1 μM) to give 25 equiv. Then, Cys (2.6 mg, 0.02 mmol) was dissolved in bis-tris buffer (10 mM, 1 mL) and 1.5-15 μL of this Cys solution (20 mM) were transferred to each complex solution (1 μM). After mixing them for a few seconds, fluorescence spectra were taken at room temperature.

2.4. UV-vis titration

For Hg^{2+}, **1** (1.4 mg, 0.005 mmol) was dissolved in methanol (1 mL) and 3.0 μL of this solution (5 mM) were diluted with 3 mL of 10 mM bis-tris buffer to make the final concentration of 5 μM. $Hg(NO_3)_2{\cdot}H_2O$ (1.7 mg, 0.005 mmol) was dissolved in DMF (1 mL) and 0.3-3 μL of this Hg^{2+} solution (5 mM) were transferred to each receptor solution (5 μM).

After mixing them for a few seconds, UV-vis spectra were taken at room temperature.

For Cys, **1** (1.4 mg, 0.005 mmol) was dissolved in methanol (1 mL) and 3.0 μL of this solution (5 mM) were diluted with 3 mL of 10 mM bis-tris buffer to make the final concentration of 5 μM. $Hg(NO_3)_2 \cdot H_2O$ (1.7 mg, 0.005 mmol) was dissolved in DMF (1 mL) and 1.8 μL of this Hg^{2+} solution (5 mM) were transferred to each receptor solution (5 μM) to give 0.6 equiv. Then, Cys (2.6 mg, 0.02 mmol) was dissolved in bis-tris buffer (10 mM, 1 mL) and 1.5-25.5 μL of this Cys solution (20 mM) were transferred to each complex solution (5 μM). After mixing them for a few seconds, UV-vis spectra were taken at room temperature.

2.5. Job plot measurements

For Hg^{2+}, **1** (1.4 mg, 0.005 mmol) was dissolved in methanol (1 mL). 60, 54, 48, 42, 36, 30, 24, 18, 12, 6 and 0 μL of the **1** solution were taken and transferred to vials. Each vial was diluted with bis-tris buffer to make a total volume of 2.940 mL. $Hg(NO_3)_2 \cdot H_2O$ (1.7 mg, 0.005 mmol) was dissolved in DMF (1 mL). 0, 6, 12, 18, 24, 30, 36, 42, 48, 54, and 60 μL of the $Hg(NO_3)_2$ solution were added to each diluted **1** solution. Each vial had a total volume of 3 mL. After reacting them for a few seconds, fluorescence spectra were taken at room temperature.

For Cys, **1** (2.8 mg, 0.01 mmol) was dissolved in methanol (1 mL) and $Hg(NO_3)_2 \cdot H_2O$ (1.7 mg, 0.005 mmol) was dissolved in DMF (1 mL), respectively. The two solutions were mixed to make Hg^{2+}-2·**1** complex. 30, 27, 24, 21, 18, 15, 12, 9, 6, 3 and 0 μL of the Hg^{2+}-2·**1** solution were taken and transferred to vials. Each vial was diluted with bis-tris buffer to make a total volume of 2.97 mL. Cys (0.65 mg, 0.005 mmol) was dissolved in bis-tris buffer (10 mM, 1 mL). 0, 3, 6, 9, 12, 15, 18, 21, 24, 27, and 30 μL of the Cys solution were added to each diluted Hg^{2+}-2·**1** solution. Each vial had a total volume of 3 mL. After reacting them for a few seconds, fluorescence spectra were taken at room temperature.

2.6. Competition experiments

For Hg^{2+}, **1** (1.4 mg, 0.005 mmol) was dissolved in methanol (1 mL) and 0.6 μL of this solution (5 mM) were diluted with 2.970 mL of 10 mM bis-tris buffer to make the final concentration of 1 μM. MNO_3 (M = Na, K, Ag, 0.005 mmol) or $M(NO_3)_2$ (M = Mn, Co, Ni,

Cu, Zn, Cd, Mg, Ca, Pb, 0.005 mmol) or $M(ClO_4)_2$ (M = Fe, 0.005 mmol) or $M(NO_3)_3$ (M = Fe, Cr, Al, Ga, In, 0.005 mmol) were separately dissolved in 10 mM bis-tris (1 mL). 15 μL of each metal solution (5 mM) were taken and added to 3 mL of the solution of receptor **1** (1 μM) to give 25 equiv of metal ions. Then, 15 μL of Hg^{2+} solution (5 mM) were added into the mixed solution of each metal ion and **1** to make 25 equiv. After mixing them for a few seconds, fluorescence spectra were taken at room temperature.

For Cys, **1** (1.4 mg, 0.005 mmol) was dissolved in methanol (1 mL) and 0.6 μL of the **1** (5 mM) were diluted to 2.964 mL of 10 mM bis-tris buffer to make the final concentration of 1 μM. $Hg(NO_3)_2{\cdot}H_2O$ (1.7 mg, 0.005 mmol) was dissolved in DMF (1 mL). 15 μL of Hg^{2+} solution (5 mM) was taken and added into **1** solution (1 μM) to make mercury complex. Various amino acids and peptide such as Ala, Asn, Cys, Gln, Glu, Gly, His, Ile, Leu, Lys, Met, Phe, Pro, Ser, Trp, Val, Arg, Thr, Asp and glutathione (GSH) (0.02 mmol) were separately dissolved in 10 mM bis-tris buffer (20 mM). 10.5 μL of each amino acid and peptide solution (20 mM) were taken and added into each mercury complex solution prepared above to make 70 equiv. Then, 10.5 μL of the Cys solution (20 mM) were added into the mixed solution of each amino acid or peptide and mercury complex to make 70 equiv. After mixing them for a few minutes, fluorescence spectra were taken at room temperature.

2.7. pH effect test

A series of buffers with pH values ranging from 2 to 12 was prepared by mixing sodium hydroxide solution and hydrochloric acid in bis-tris buffer. After the solution with a desired pH was achieved, receptor **1** (1.4 mg, 0.005 mmol) was dissolved in methanol (1mL), and then 0.6 μL of the receptor **1** (5 mM) was diluted with 3.0 mL of 10 mM bis-tris buffer to make the final concentration of 1 μM. $Hg(NO_3)_2{\cdot}H_2O$ (1.7 mg, 0.005 mmol) was dissolved in DMF (1 mL). 15 μL of the Hg^{2+} solution (5 mM) were transferred to each receptor solution (1 μM) prepared above. After reacting them for a few seconds, fluorescence spectra were taken at room temperature.

2.8. ^{1}H NMR titration of **1** with Hg^{2+}

For ^{1}H NMR titration of receptor **1** with Hg^{2+}, three NMR tubes of receptor **1** (2.74 mg, 0.01 mmol) dissolved in DMF-d_7 (700 μL) were prepared and then three different

concentrations (0, 0.0025, and 0.005 mmol) of $Hg(NO_3)_2 \cdot H_2O$ dissolved in DMF-d_7 were added to each solution of receptor **1**. After shaking them for a minute, ^{1}H NMR spectra were obtained at room temperature.

2.9. Determination of Hg^{2+} in water samples.

Fluorescence spectral measurements of water samples containing Hg^{2+} were carried by adding 3 μL of 1 mM stock solution of **1** and 0.60 mL of 50 mmol/L bis-tris buffer stock solution to 2.397 mL sample solutions. After well mixed, the solutions were allowed to stand at 25 ˚C for 2 min before the test.

2.10. Theoretical calculations methods

All DFT/TDDFT calculations based on the hybrid exchange-correlation functional B3LYP[43,44] were carried out using Gaussian 03 program.[45] The 6-31G** basis set[46,47] was used for the main group elements, whereas the Lanl2DZ effective core potential (ECP)[48-50] was employed for Hg^{2+}. In vibrational frequency calculations, there was no imaginary frequency for the optimized geometries of **1** and Hg^{2+}-2·**1** complex, suggesting that these geometries represented local minima. For all calculations, the solvent effect of water was considered by using the Cossi and Barone's CPCM (conductor-like polarizable continuum model).[51,52] To investigate the electronic properties of singlet excited states, time-dependent DFT (TDDFT) was performed in the ground state geometries of **1** and Hg^{2+}-2·**1** complex. The 30 singlet-singlet excitations were calculated and analyzed. The GaussSum 2.1[53] was used to calculate the contributions of molecular orbitals in electronic transitions.

3. Results and discussion

3.1. Synthesis of receptor **1**

Receptor **1** was obtained by the combination of benzene-1,2-diamine and 6-bromopyridine-2-carboxaldehyde with 54 % yield in ethanol (Scheme 1), and characterized by ^{1}H NMR and ^{13}C NMR, ESI-mass spectroscopy, and elemental analysis.

3.2. Fluorescent turn-off detection of Hg^{2+}

The fluorescence response of **1** toward 19 different metal ions (Ag^{+}, Al^{3+}, Ca^{2+}, Cd^{2+}, Co^{2+}, Cr^{3+}, Cu^{2+}, Fe^{2+}, Fe^{3+}, Ga^{3+}, Hg^{2+}, In^{3+}, K^{+}, Mg^{2+}, Mn^{2+}, Na^{+}, Ni^{2+}, Pb^{2+}, and Zn^{2+}) was measured in a bis-tris buffer solution (10 mM, pH 7.0) (Fig. 1). Compound **1** exhibited a characteristic fluorescence emission band at 395 nm (λ_{ex} = 320 nm). Upon the addition of 25 equiv of each metal ion, only Hg^{2+} induced a remarkable fluorescence quenching while other metal ions showed either no or some change in the emission intensity relative to the free receptor **1**. For example, Cd^{2+}, Al^{3+}, Ga^{3+} and Co^{2+} showed to some extent decrease of the intensity in comparison with **1**. These results suggested that the receptor **1** could be a good fluorescence chemosensor for Hg^{2+}.

To understand the binding affinity of **1** towards Hg^{2+}, the emission titration studies have been performed (Fig. 2). Upon the gradual addition of Hg^{2+} up to 25 equiv, about 90 % of the maximum fluorescence intensity was quenched. The binding properties of **1** with Hg^{2+} were further studied by UV-vis titration experiments (Fig. 3). On the treatment with Hg^{2+} to the solution of **1**, the absorbance at 310 nm gradually decreased, whereas a new band at 364 nm steadily increased until the amounts of Hg^{2+} reached approximately 0.6 equiv. The isosbestic point was observed at 333 nm, demonstrating that only one product was generated from the interaction of **1** with Hg^{2+}.

In order to understand the binding stoichiometry of receptor **1** and Hg^{2+}, Job plot analysis was carried out (Fig. S1). The emission intensity at 395 nm was plotted against the molar fraction of **1** under a constant total concentration of **1** and Hg^{2+}. The result indicated a 1:2 ratio for Hg^{2+} to **1**. In addition, the formation of a 1:2 complex was confirmed using ESI-mass spectrometry (Fig. S2). The positive-ion mass spectrum indicated that a peak at m/z = 746.80 was assignable to $[Hg^{2+} + 2\cdot\mathbf{1}(-H^{+})]^{+}$ [calcd. 746.94].

To get further information for the binding mode of **1** with Hg^{2+}, ^{1}H NMR titration study was carried out (Fig. S3). Upon the addition of 0.5 equiv of Hg^{2+} to **1**, the NH peak of the benzimidazole moiety at 13.3 ppm completely disappeared, indicating that the N atom of the NH moiety might bind to Hg^{2+}. In addition, all the proton signals of the benzimidazole moiety and pyridine ring showed a significant downfield shift. These results suggested that the N atom of pyridine moiety might coordinate to Hg^{2+}. The peaks did not changed upon further addition of Hg^{2+}. Based on Job plot, ESI-mass spectrometry analysis and ^{1}H NMR

titration, we proposed the structure of Hg^{2+}-2·**1** complex as shown in Scheme 2.

The association constant of Hg^{2+} binding to sensor **1** was found to be 5.0 x 10^{10} M^{-2} on the basis of Li's equation (Fig. S4).[54] This value clearly indicated that **1** had a strong binding affinity to Hg^{2+} in buffer solution. The detection limit of senor **1** as a fluorescent sensor for the detection of Hg^{2+} was determined from a plot of fluorescent intensity as a function of the concentration of Hg^{2+}. It was found that chemosensor **1** had a detection limit of 0.74 μM on the basis of 3σ/K (Fig. S5).[55]

The preferential selectivity of **1** as a fluorescent chemosensor for the detection of Hg^{2+} was studied in the presence of various competing metal ions. For competitive studies, receptor **1** was treated with 25 equiv of Hg^{2+} in the presence of 25 equiv of other metal ions, as indicated in Fig. 4. There was no interference for detection of Hg^{2+} in the presence of Ag^{+}, Al^{3+}, Ca^{2+}, Cd^{2+}, Co^{2+}, Cr^{3+}, Cu^{2+}, Fe^{2+}, Fe^{3+}, Ga^{3+}, In^{3+}, K^{+}, Mg^{2+}, Mn^{2+}, Na^{+}, Ni^{2+}, Pb^{2+}, and Zn^{2+}. Thus, the receptor **1** could be used as an excellent fluorescent sensor for Hg^{2+} in the presence of most competing metal ions.

The effect of pH between chemosensor **1** and Hg^{2+} ion was investigated at a pH range from 2 to 12 (Fig. S6). The Hg^{2+}-2·**1** complex showed a significant fluorescence response between pH 7 and 12, which includes the environmentally relevant range of pH 7.0 - 8.4.[56] These results indicated that Hg^{2+} could be clearly detected by the fluorescence spectral measurement using **1** within the environmental pH range.

In order to examine the applicability of the chemosensor **1** in environmental samples, we constructed a calibration curve for the determination of Hg^{2+} by **1** (Fig. S7), which exhibited a good linear relationship between the fluorescence intensity of **1** and Hg^{2+} concentration (1.0-10.00 μM) with a correlation coefficient of R^2 = 0.991 (n = 3). Then, the chemosensor was applied for the determination of Hg^{2+} in water samples. We prepared artificial polluted water samples by adding various metal ions known as being in industrial processes into deionized water. The results were summarized in Table 1, which exhibited a satisfactory recovery and R.S.D. values for the water samples.

3.3 Theoretical calculations of **1** with Hg^{2+}

To understand the sensing mechanisms of Hg^{2+} with **1**, theoretical calculations were performed in parallel to the experimental studies. As Job plots, ESI-mass spectrometry analysis and NMR titration showed that **1** reacted with Hg^{2+} in the 2:1 (L:M) stoichiometric ratio, all theoretical calculations were performed with the 2:1 stoichiometry. Hg^{2+}-2·**1** complex was optimized with a diamagnetic character (S=0, DFT/B3LYP/main group atom: 6-31G** and Hg: Lanl2DZ/ECP). The significant structural properties of the energy-minimized structures were shown in Fig. S8.

We also investigated the absorption to the singlet excited states of **1** and Hg^{2+}-2·**1** species via TDDFT calculations. In case of **1**, the main molecular orbital (MO) contribution of the first lowest excited state was determined for HOMO → LUMO transition (317.90 nm, Fig. S9), which indicated π→π* transition band. Therefore, the turn-on fluorescence of **1** could be due to the π→π* transition band. On the other hand, in case of Hg^{2+}-2·**1** complex, the first, second and third excited states (342.03, 341.05 and 338.24 nm) indicated that most MO contributions of π→π* transitions were delocalized and the oscillator strengths were lower than those of **1**, which affect the turn-off fluorescence of Hg^{2+}-2·**1** complex (Fig. S10). Moreover, it has been suggested that the heavy metal ion such as Hg^{2+} with a high spin-orbit coupling constant (ζ) stabilize the triplet state and effectively quench the fluorescence.[57,58] Therefore, we assumed that the fluorescence quenching mechanism of **1** by Hg^{2+} might be due to the delocalization of π→π* transitions by the chelation of Hg^{2+} with **1** and the high spin-orbit coupling constant of Hg^{2+}.

3.4. Fluorescent turn-on response of Hg^{2+}-2·**1** complex toward Cys

Based on the thiophilic nature of Hg^{2+}, we examined the selectivity of Hg^{2+}-2·**1** complex toward Cys. The fluorescent spectral study of Hg^{2+}-2·**1** complex with 20 different amino acids and peptide such as Ala, Asn, Cys, Gln, Glu, Gly, His, Ile, Leu, Lys, Met, Phe, Pro, Ser, Trp, Val, Arg, Thr, Asp and GSH was carried out in bis-tris buffer solution (Fig. 5). Only the addition of Cys into the solution of Hg^{2+}-2·**1** enhanced significantly the intensity of fluorescence emission while other amino acids showed either no or slight change in the emission spectra relative to the free receptor **1**. For example, GSH showed a slight increase of the emission intensity, and Trp quenched it. The fluorescence recovery might be due to release of **1** from the Hg^{2+}-2·**1** complex through the interaction of thiol-containg Cys with

Hg^{2+}. These results showed that Hg^{2+}-2·**1** complex was successfully utilized to probe Cys with turn-on of fluorescence, and could selectively recognize cysteine over other sulfur-containing amino acid and peptide, such as Met and GSH. Importantly, this is the second example of Cys-selective fluorescent chemosensor by using mercury complex as a receptor in fully aqueous solution, to the best of our knowledge (Table S1).

To investigate the sensing properties of Cys by Hg^{2+}-2·**1** complex, fluorescence titration was conducted in buffer solution (Fig. 6). On the treatment with Cys to the solution of Hg^{2+}-2·**1**, the fluorescence intensity enhanced gradually and saturated when the concentration of Cys reached 70 equiv. The absorbance change of Hg^{2+}-2·**1** with Cys was studied by UV-vis titration experiments (Fig. 7). Upon the addition of Cys into the solution of Hg^{2+}-2·**1**, the absorption band at 364 nm steadily decreased, and a band at 310 nm gradually increased. The final UV-vis spectrum was nearly identical to that of sensor **1**, indicating release of **1** from the Hg^{2+}-2·**1** complex. Meanwhile, the isosbestic points were observed at 282 and 331 nm, which indicates the formation of a single species from Hg^{2+}-2·**1** complex upon binding to Cys.

Job plot showed a 1:2 stoichiometric ratio of Hg^{2+}-2·**1** to Cys (Fig. S11). In addition, the 1:2 stoichiometry between the Hg^{2+}-2·**1** and Cys was confirmed by ESI-mass spectrometry analysis (Fig. S12). The positive ion mass spectrum showed that a peak at m/z = 274.20 was assignable to [**1** + H^+]$^+$ [cald, 274.00], resulting in release of **1** from Hg^{2+}-2·**1** complex. Moreover, the peak of [Hg^{2+} + 2·Cys + H^+]$^+$ was observed at [m/z 442.93; calcd 443.00], indicating the 1:2 binding mode between Hg^{2+} and Cys. Based on Job plot, UV-vis titrations, and ESI-mass spectrometry analysis, we proposed that a Hg^{2+}-2·**1** complex might undergo the demetallation by two Cys to form Hg^{2+}-2·Cys complex (Scheme 3). The binding constant between Hg^{2+}-2·**1** and Cys was calculated as 4.2 x 10^2 M^{-2} on the basis of Li's equation (Fig. S13).[54] Based on the result of fluorescence titration, the detection limit for Cys was determined to be 5.2 μM on basis of 3σ/K (Fig. S14).[55]

The practical applicability of Hg^{2+}-2·**1** complex as a Cys-selective receptor was further ascertained by the competition experiment (Fig. 8). When **1** was treated with 70 equiv of Cys in the presence of the same concentration of other amino acids and peptide, the emission enhancement caused by Cys was retained with Asn, Gln, Glu, Ile, Leu, Lys, Met,

Phe, Pro, Ser, Trp, Arg, and GSH. Instead, Ala, Gly, His, Val, Thr and Asp showed about 30-50% reduction of the intensity. Nevertheless, **1** still had sufficient "turn-on" fluorescence for the detection of Cys in the presence of Ala, Gly, His, Val, Thr and Asp. Therefore, these results demonstrated that Hg^{2+}-2·**1** could be an excellent fluorescent sensor with high selectivity for Cys over competing amino acids and sulfur-containing substances in buffer solution.

4. Conclusion

We have developed the simple and easy-to-make benzimidazole-based fluorescent chemosensor **1**, which showed an excellent sequential selectivity for Hg^{2+} and Cys in fully aqueous solution. In the presence of Hg^{2+}, the fluorescent receptor **1** would form Hg^{2+}-2·**1** complex, which induces a dramatic fluorescence quenching. Moreover, the chemo-sensing ensemble Hg^{2+}-2·**1** was used as a fluorescent turn-on sensor for Cys using the property of the mercury-sulfur affinity. Importantly, **1** is the second example of fluorescent chemosensor for the sequential detection of Hg^{2+} and Cys in water. Furthermore, recovery studies of the water samples added with Hg^{2+} demonstrated its value in the practical application. Therefore, we believe that the chemosensor **1** could be a good guidance to the development of a new type of the sequential recognition of Hg^{2+} and Cys.

Acknowledgements

Basic Science Research Program through the National Research Foundation of Korea (NRF) funded by the Ministry of Education, Science and Technology (NRF-2014R1A2A1A11051794, 2012001725 and 2012008875) and Daesang are gratefully acknowledged. We thank Nano-Inorganic Laboratory, Department of Nano & Bio Chemistry, Kookmin University to access the Gaussian 03 program packages.

Supplementary information

Supplementary material associated with this article can be found, in the online version.

References

1 M. F. Wolfe, S. Schwarbach and R. A. Sulaiman, *Environ. Toxicol. Chem.*, 1998, **17**, 146-148.

2 A. Ojida, H. Nonaka, Y. Miyahara, S. Tamaur, K. Sada and I. Hamachi, *Angew. Chem.*, 2006, **118**, 5564-5647.

3 J. S. Kim, M. G. Choi, K. C. Song, K. T. No, S. Ahn and S. K. Chang, *Org. Lett.*, 2007, **9**, 1129-1132.

4 P. G. Jiang, L. Z. Chen, J. Lin, Q. Liu, J. Ding, X. Gao and Z. J. Guo, *Chem. Commun.*, 2002, **13**, 1424-1425.

5 H. Y. Jo, G. J. Park, Y. J. Na, Y. W. Choi, G. R. You and C. Kim, *Dyes Pigm.*, 2014, **109**, 127-134.

6 S. Yoon, E. W. Miller, Q. He, P. H. Do and C. J. Chang, *Angew. Chem. Int. Ed.*, 2007, **46**, 6658-6661.

7 S. H. Kim, J. S. Kim, S. M. Park and S. K. Chang, *Org. Lett.*, 2006, **8**, 371-374.

8 G. J. Park, I. H. Hwang, E. J. Song, H. Kim and C. Kim, *Tetrahedron*, 2013, **70**, 2822-2828.

9 R. Martinez, F. Zapata, A. Caballero, A. Espinosa, A. Tairraga and P. Molina, *Org. Lett.*, 2006, **8**, 3235-3238.

10 S. Y. Moon, N. R. Cha, Y. H. Kim and S. K. Chang, *J. Org. Chem.*, 2004, **69**, 181-183.

11 H. H. Harris, I. J. Pickering and G. N. George, *Science*, 2003, **301**, 1203.

12 N. Zheng, Q. C. Wang, X. W. Zhang, D. M. Zheng, Z. S. Zhang and S. Q. Zhang, *Sci. Total. Environ.*, 2007, **387**, 96-104.

13 M. H. Lee, B. K. Cho, J. Yoon and J. S. Kim, *Org. Lett.*, 2007, **9**, 4515-4518.

14 Y. W. Choi, G. R. You, M. M. Lee, J. Kim, K. D. Jung and C. Kim, *Inorg. Chem. Commun.*, 2014, **46**, 43-46.

15 P. B. Tchounwou, W. K. Ayensu, N. Ninashvili and D. Sutton, *Environ. Toxicol.*, 2003, **18**, 149-175.

16 J. Gutknecht, *J. Membr. Biol.*, 1981, **61**, 61-66.

17 D. Joshi, D. K. Mittal, S. Shukla and A. K. Srivastav, *Exp. Toxicol. Pathol.*, 2012, **64**, 103-108.

18 L. Tamer, G. Yucebilgic, R. Bilgin, K. Tanriverdi and S. S. Tukel, *Biochem. Arch.*, 1998, **14**, 207-210.

19 N. Zhang, G. Li, Z. Cheng and X. Zuo, *J. Hazard. Mater.*, 2012, **229-230**, 404-410.

20 J. H. Soh, K. M. K. Swamy, S. K. Kim, S. Kim, S. H. Lee and J. Yoon, *Tetrahedron Lett.*, 2007, **48**, 5966-5969.

21 J. H. Kim, J. Y. Noh, I. H. Hwang, J. J. Lee and C. Kim, *Tetrahedron Lett.*, 2013, **54**, 4001-4005.

22 S. Seshadri, A. Beiser, J. P. Selhub, F. I. Jacques, H. Rosenberg, R. B. D'Agostino, P. W. Wilson and P. A. N. Wolf, *Engl. J. Med.*, 2002, **346**, 476-483.

23 S. A. Lee, J. J. Lee, J. W. Shin, K. S. Min and C. Kim, *Dyes Pigm.*, 2015, **116**, 131-138.

24 Y. Yang, F. J. Huo, C. Yin, J. Chao and Y. Zhang, *Dyes Pigm.*, 2015, **114**, 105-109.

25 C. Hwang, A. J. Sinskey and H. F. Lodish, *Science*, 1992, **257**, 1496-1502.

26 L. Wang, Q. Zhou, B. Zhu, L. Yan, Z. Ma, B. Du and X. Zhang, *Dyes Pigm.*, 2012, **95**, 275-279.

27 S. Shahrokhian, *Anal. Chem.*, 2001, **73**, 5972-5978.

28 Y. S. Kim, G. J. Park, S. A. Lee and C. Kim, *RSC Adv.*, 2015, **5**, 31179-31188.

29 D. W. Jacobsen, *Clin. Chem.*, 1998, **44**, 1833-1843.

30 L. P. Duan, Y. F. Xu, X. H. Qian, F. Wang, J. W. Liu and T. Y. Cheng, *Tetrahedron Lett.*, 2008, **49**, 6624-6627.

31 O. Rusin, N. N. Luce, R. A. Agbaria, J. O. Escobedo, S. Jiang, I. M. Warner, F. B. Dawan, K. Lian and R. M. Strongin, *J. Am. Chem. Soc.*, 2004, **126**, 438-439.

32 W. H. Wang, O. Rusin, X. Y. Xu, K. K. Kim, J. O. Escobedo, S. O. Fakayode, K. A. Fletcher, M. Lowry, C. M. Schowalter, C. M. Lawrence, F. R. Fronczek, I. M. Warner and R. M. Strongin, *J. Am. Chem. Soc.*, 2005, **127**, 15949-15958.

33 A. R. Ivanov, I. V. Nazimov and L. A. Baratova, *J. Chromatogr. A*, 2000, **870**, 433-442.

34 A. R. Ivanov, I. V. Nazimov and L. Baratova, *J. Chromatogr. A.*, 2000, **895**, 157-166.

35 T. Inoue and J. R. Kirchhoff, *Anal. Chem.*, 2000, **72**, 5755-5760.

36 M. Wen, H. Liu, F. Zhang, Y. Z. Zhu, D. Liu, Y. Tian and Q. Wu, *Chem. Commun.*, 2009, **30**, 4530-4532.

37 Z. Guo, W. Zhu and H. Tian, *Marcromolecules.*, 2010, **43**, 739-744.

38 X. Chen, S. W. Nam, M. J. Jou, Y. Kim, S. J. Kim, S. Park and J. Yoon, *Org. Lett.*, 2008, **10**, 5235-5338.

39 Q. Zou, X. Li, J. Zhang, J. Zhou, B. Sun and H. Tian, *Chem. Commun.*, 2012, **48**, 2095-2097.

40 S. Madhu, D. K. Sharma, S. K. Basu, S. Jadhav, A. Chowdhury and M. Ravikanth, *Inorg. Chem.*, 2013, **52**, 11136-11345.

41 N. Singh and D. O. Jang, *Org. Lett.*, 2007, **9**, 1991-1994.

42 P. Molina, A. Tarraga and F. Oton, *Org. Biomol. Chem.*, 2012, **10**, 1711-1724.

43 A. D. Becke, *J. Chem. Phys.*, 1993, **98**, 5648-5652.

44 C. Lee, W. Yang and R. G. Parr, *Phys. Rev. B*, 1988, **37**, 785-789.

45 M. J. Frisch, G. W. Trucks, H. B. Schlegel, G. E. Scuseria, M. A. Robb, J. R. Cheeseman, J. A. Montgomery, Jr., T. Vreven, K. N. Kudin, J. C. Burant, J. M. Millam, S. S. Iyengar, J. Tomasi, V. Barone, B. Mennucci, M. Cossi, G. Scalmani, N. Rega, G. A. Petersson, H. Nakatsuji, M. Hada, M. Ehara, K. Toyota, R. Fukuda, J. Hasegawa, M. Ishida, T. Nakajima, Y. Honda, O. Kitao, H. Nakai, M. Klene, X. Li, J. E. Knox, H. P. Hratchian, J. B. Cross, V. Bakken, C. Adamo, J. Jaramillo, R. Gomperts, R. E. Stratmann, O. Yazyev, A. J. Austin, R. Cammi, C. Pomelli, J. W. Ochterski, P. Y. Ayala, K. Morokuma, G. A. Voth, P. Salvador, J. J. Dannenberg, V. G. Zakrzewski, S. Dapprich, A. D. Daniels, M. C. Strain, O. Farkas, D. K. Malick, A. D. Rabuck, K. Raghavachari, J. B. Foresman, J. V. Ortiz, Q. Cui, A. G. Baboul, S. Clifford, J. Cioslowski, B. B. Stefanov, G. Liu, A. Liashenko, P. Piskorz, I. Komaromi, R. L. Martin, D. J. Fox, T. Keith, M. A. Al-Laham, C. Y. Peng, A. Nanayakkara, M. Challacombe, P. M. W. Gill, B. Johnson, W. Chen, M. W. Wong, C. Gonzalez, and J. A. Pople, Gaussian 03, Revision D.01, Gaussian, Inc., Wallingford CT, 2004.

46 P. C. Hariharan and J. A. Pople, *Theor. Chim. Acta*, 1973, **28**, 213-222.

47 M. M. Francl, W. J. Petro, W. J. Hehre, J. S. Binkley, M. S. Gordon, D. F. DeFrees and J. A. Pople, *J. Chem. Phys.*, 1982, **77**, 3654-3665.

48 P. J. Hay and W. R. Wadt, *J. Chem. Phys.*, 1985, **82**, 270-283.

49 P. J. Hay and W. R. Wadt, *J. Chem. Phys.*, 1985, **82**, 284-298.

50 P. J. Hay and W. R. Wadt, *J. Chem. Phys.*, 1985, **82**, 299-310.

51 V. Barone and M. Cossi, *J. Phys. Chem. A*, 1998, **102**, 1995-2001.

52 M. Cossi and V. Barone, *J. Chem. Phys.*, 2001, **115**, 4708-4717.

53 N. M. O'boyle, A. L. Tenderholt and K. M. Langner, *J. Comput. Chem.*, 2008, **29**, 839-845.

54 G. Grynkiewcz, M. Poenie and R. Y. Tsein, *J. Biol. Chem.*, 1985, **260**, 3440-3445.

55 Y. K. Tsui, S. Devaraj and Y. P. Yen, *Sens. Actuators, B*, 2012, **161**, 510-519.

56 R. M. Harrison, D. P. H. Laxen and S. J. Wilson, *Environ. Sci. Technol.*, 1981, **15**, 1378-1383.

57 D. S. McClure, *J. Chem. Phys.*, 1949, **17**, 905-913.

58 K. N. Solovyov and E. A. Borisevich, *Physics-Uspekhi*, 2005, **48**, 231-253.

59 A. Thangaraj, S. Gandhi and C. Duraisamy, *Spectrochim. Acta Part A*, 2014, **123**, 18-24.

60 L. Chao, Z. Qianxiong, Z. Baowen and W. Xuesong, *New J. Chem.*, 2011, **35**, 45-48.

61 A. K. Mahapatra, J. Roy, P. Sahoo, S. K. Mukhopadhyay, A. Banik and D. Mandal, *Tetrahedron Lett.*, 2013, **54**, 2946-2951.

62 Q. Lin, H. Yangwei, F. Juan, W. Ruyong and F. Nanyan, *Talanta*, 2013, **114**, 66-72.

63 H. P. Fang, M. Shellaiah, A. Singh, M. V. R. Raju, Y. H. Wu and H. C. Lin, *Sens. Actuators, B*, 2014, **194**, 229-237.

64 F. Geng, Y. Wang, P. Qu, Y. Zhang, H. Dong and M. Xu, *Anal. Methods*, 2013, **5**, 3965-3969.

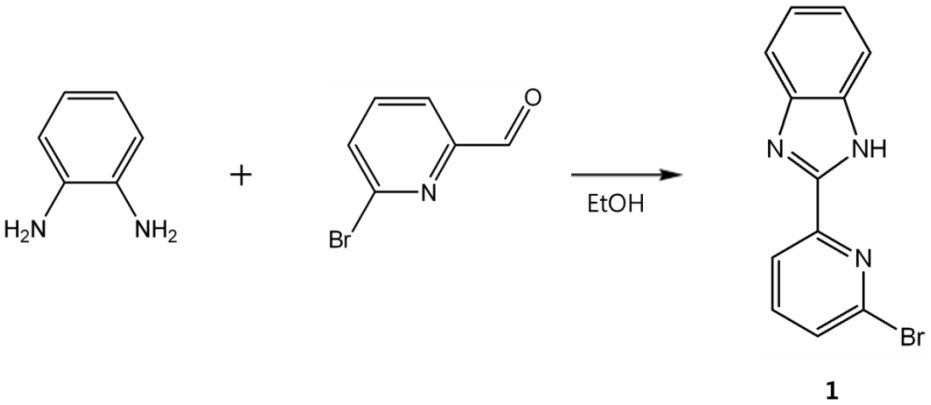

Scheme 1. Synthesis of **1**.

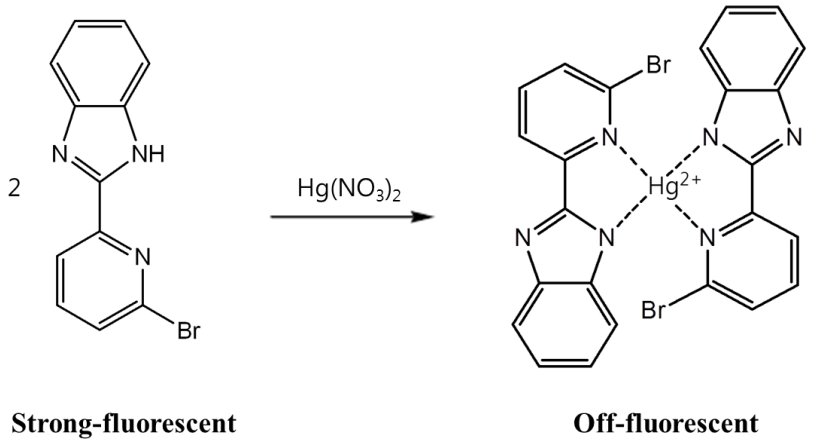

Scheme 2. Proposed binding mode of Hg^{2+}-2·**1** complex.

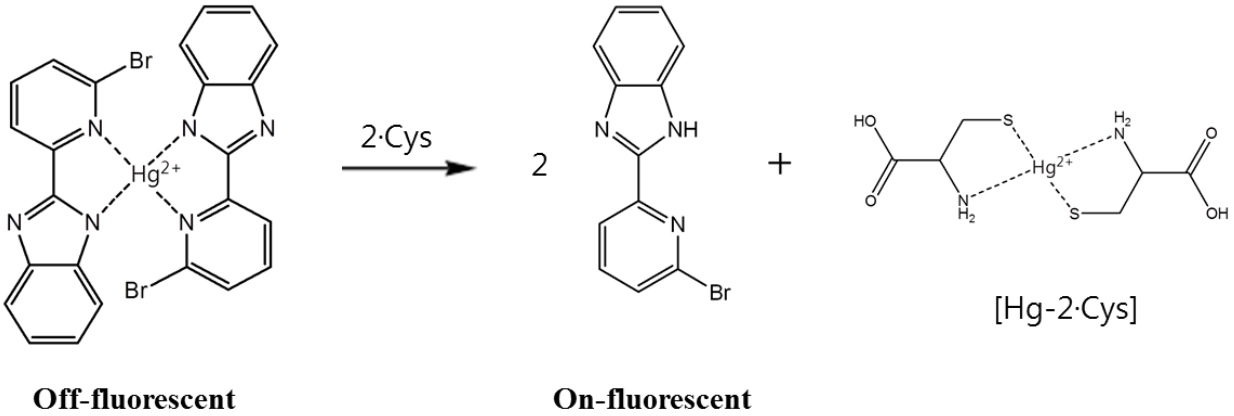

Scheme 3. Proposed sensing mechanism of Cys by Hg^{2+}-2·**1** complex.

Table 1. Determination of Hg(II) in water samples

Sample	Hg(II) added (μmol/L)	Hg(II) found (μmol/L)	Recovery (%)	R.S.D (n=3) (%)
Water Sample [a]	0.00	6.31	105.2	2.8
	2.00	8.65	108.1	2.1

[a] Synthesized by deionized water, 6.00 μmol/L Hg(II), 10 μmol/L Cd(II), Pb(II), Na(I), K(I), Ca(II), Mg(II). Conditions: [**1**] = 1 μmol/L in 10mM bis-tris buffer (pH 7.0).

Figure captions

Fig. 1 Fluorescence spectra of **1** (1 μM) upon the addition of 25 equiv of various metal ions in bis-tris buffer solution (10 mM, pH 7.0).

Fig. 2 Fluorescence spectral changes of **1** (1 μM) in the presence of different concentrations of Hg^{2+} ions in bis-tris buffer solution (10 mM, pH 7.0). Inset: Fluorescence intensity at 395 nm versus the number of equiv of Hg^{2+} added.

Fig. 3 Absorption spectral changes of **1** (1 μM) after addition of increasing amounts of Hg^{2+} in bis-tris buffer solution (10 mM, pH 7.0). Inset: Absorption at 364 nm versus the number of equiv of Hg^{2+} added.

Fig. 4 Competitive selectivity of **1** (1 μM) toward Hg^{2+} (25 equiv) in the presence of other metal ions (25 equiv) in bis-tris buffer solution (10 mM, pH 7.0).

Fig. 5 Fluorescence spectral changes of Hg^{2+}-2·**1** upon addition of 70 equiv of various amino acids and peptide.

Fig. 6 Fluorescence spectral changes of Hg^{2+}-2·**1** in the presence of different concentrations of Cys in bis-tris buffer solution (10 mM, pH 7.0). Inset: Fluorescence intensity at 395 nm versus the number of equiv of Cys added.

Fig. 7 Absorption spectral changes of Hg^{2+}-2·**1** after addition of increasing amounts of Cys in bis-tris buffer solution (10 mM, pH 7.0). Inset: Absorption at 364 nm versus the number of equiv of Cys added.

Fig. 8 Competitive selectivity of Hg^{2+}-2·**1** toward Cys (70 equiv) in the presence of other amino acids and peptide (70 equiv) in bis-tris buffer solution (10 mM, pH 7.0).

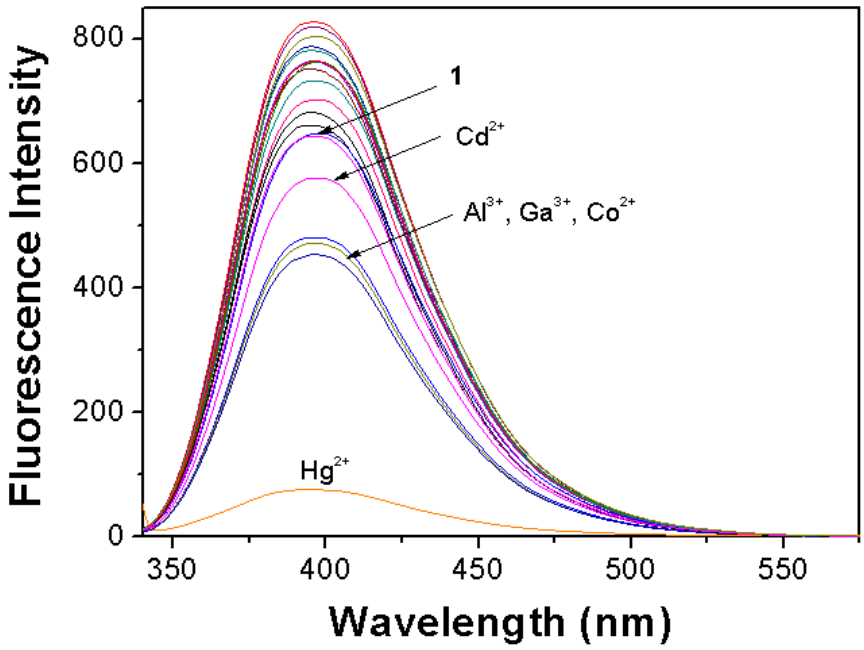

Fig. 1

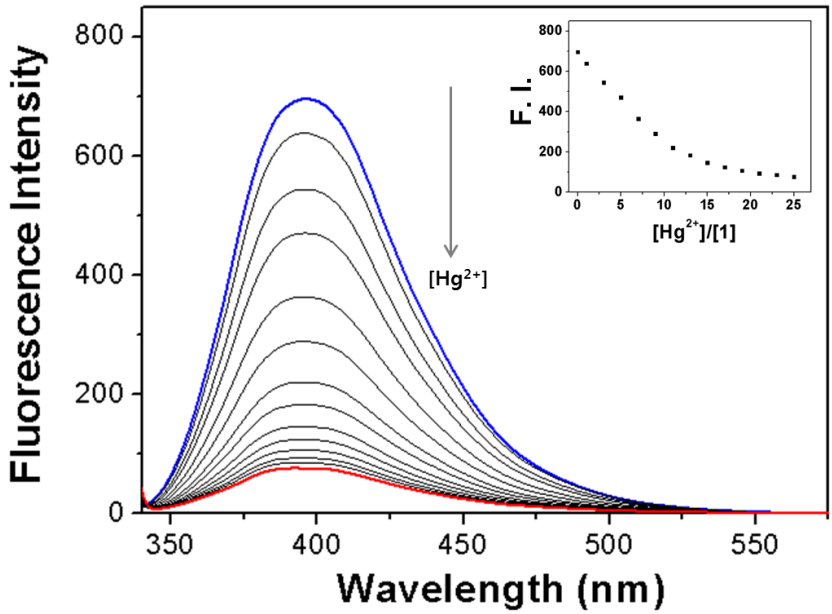

Fig. 2

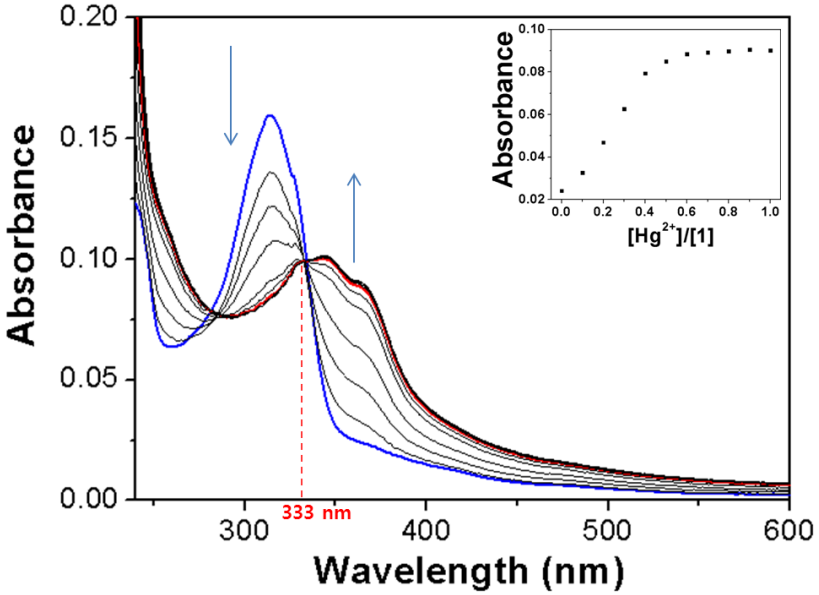

Fig. 3

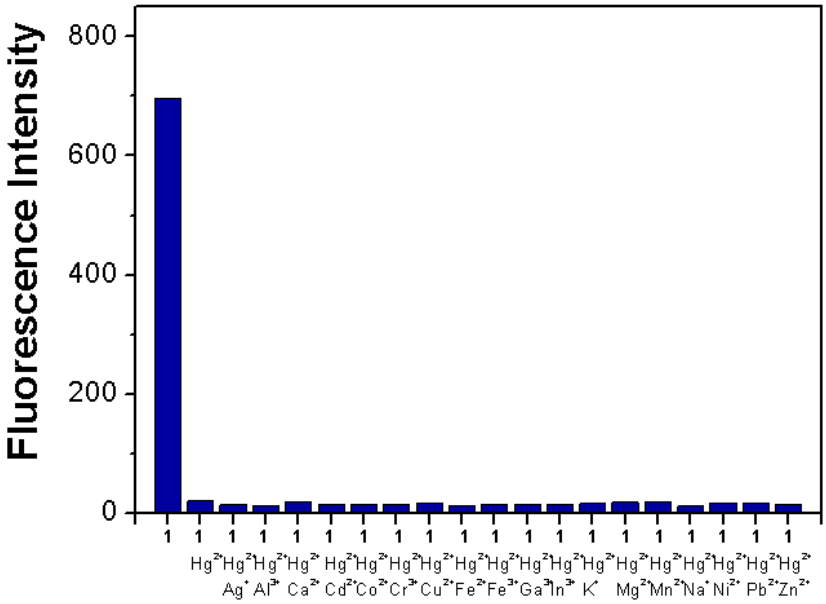

Fig. 4

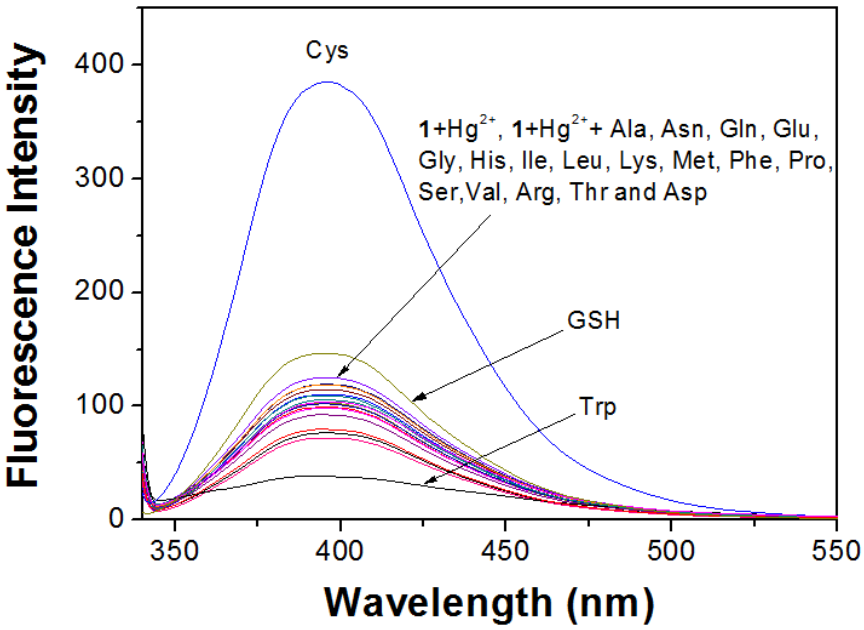

Fig. 5

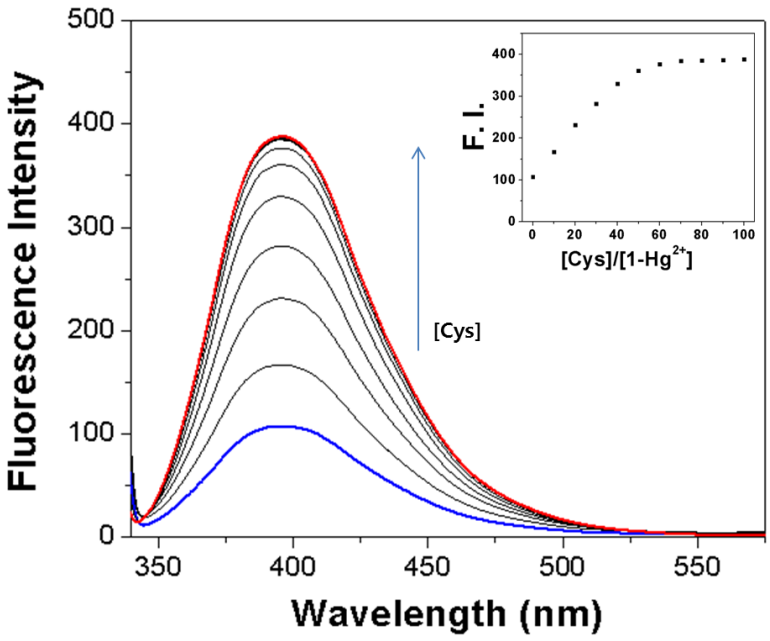

Fig. 6

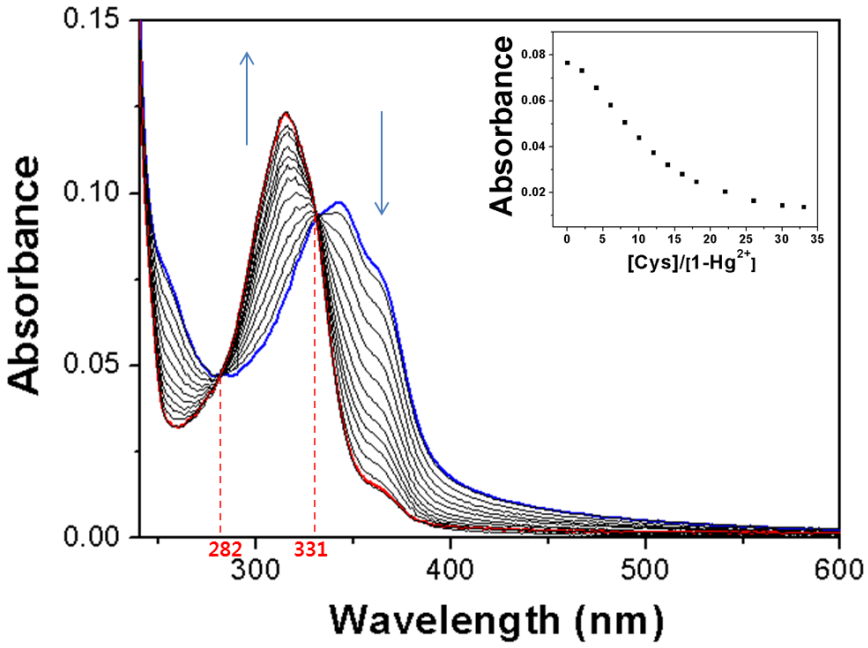

Fig. 7

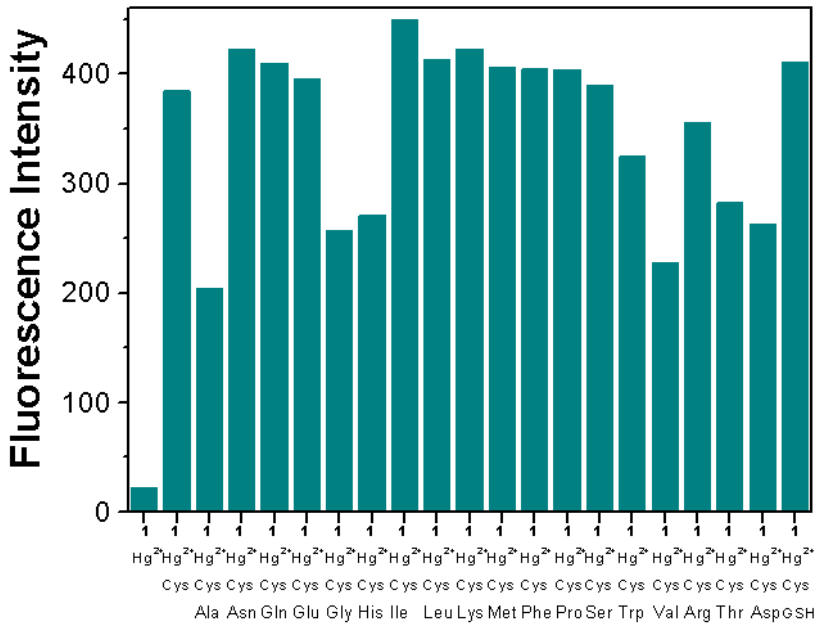

Fig. 8